A Novel Approach Analysis of Heart and Eye Disease Coherence Detection using Deep Learning Techniques

[1]Nancy Lima Christy S and [2]Nithyakalyani S
[1,2]Department of Computer Science and Engineering, KGiSL Institute of Technology, Coimbatore, Tamil Nadu, India.
[1]nancybalaji1977@gmail.com, [2]nithyakalyani.me@gmail.com

Correspondence should be addressed to Nancy Lima Christy S: nancybalaji1977@gmail.com

Article Info
Journal of Machine and Computing (https://anapub.co.ke/journals/jmc/jmc.html)
Doi: https://doi.org/10.53759/7669/jmc202505002
Received 28 March 2024; Revised from 14 April 2024; Accepted 12 September 2024.
Available online 05 January 2025.

Abstract – One of the major factors contributing to the rising death rate is cardiovascular disease. Analyzing clinical data has made it harder to predict cardiovascular disease. To solve the aforementioned problems, an improved DenseNet model is presented in this study. The proposed approach forecasts Central Retinal Artery Occlusion (CRAO) and Coronary Artery Disease (CAD) simultaneously by using the patient's data from eye and cardiac examinations. Then, the coherence relationship is calculated with the help of Pearson's correlation coefficient for both diseases. As far as we are aware, this is the first study to use DL techniques to predict the coherence between CRAO and CAD. While predicting the CAD, Improved DenseNet 97.5% accuracy when compared with benchmarked DL models like ResNet 50 and VGG16.

Keywords – Cardiovascular Disease, Deep Learning, Median Filter, Principal Component Analysis, Generative Adversarial Network, Central Retinal Artery Occlusion, Coronary Artery Disease, Improved Densenet.

I. INTRODUCTION

For each human, Eye vision is considered to be an important sense. However, a lot of people suffered from vision damages throughout the world. At least 2.2 billion people worldwide, according to the World Health Organization (WHO), are near- or farsighted. Approximately 1 billion cases, or nearly half of them, could have been prevented or received no treatment. The most common causes of distance vision impairment or blindness in this population are glaucoma (7.7 million), diabetic retinopathy (3.9 million), age-related macular degeneration (8 million), cataracts (94 million), and refractive errors (88.4 million).

Central Retinal Artery Occlusion is one of the eye conditions that causes vision loss (CRAO). CRAO is an eye disease due to blockage of flow of blood in central retinal artery. Due to this, delivery of oxygen is stopped to the retina and the patient suffered from vision loss. The CRAO disease occur due to a small piece of cholesterol (embolus) which blocks blood flow. This occlusion may be temporary or lasts some period or permanent. Carotid artery atherosclerosis is the most commonly occurred disease among occlusion.

In a similar vein, cardiovascular disease continues to be the world's leading cause of death and poses a serious threat. More than half a billion people worldwide suffer from cardiovascular diseases, which led to roughly 20.5 million deaths in 2021—nearly a third of all deaths worldwide and a notable increase from earlier estimates of 121 million deaths related to CVDs, according to the World Heart Report 2023 [3]. The Centres for Disease Control and Prevention (2020) report that heart disease was responsible for 314,186 deaths among women and 382,776 deaths (1 in 4 deaths among men).

The three leading causes of death in the United States are hypertension, stroke, and coronary heart disease (CAD). Among them, CAD occurred due to damage of main blood vessels supplied to the heart. CAD normally occurred due to swelling and deposition of cholesterol in coronary arteries. These arteries are responsible for supplying blood, nutrients as well as oxygen to the heart.

The most prevalent kind of heart disease, coronary heart disease will be responsible for 375,476 deaths in 2021[1]. Coronary Artery Disease (CAD) affects about 5% of adults who are 20 years of age or older [2]. Notably, adults under the age of 65 accounted for about 2 out of every 10 CAD-related deaths in 2021 [1]. Still, there aren't enough methods available to forecast the likelihood of heart disease from eye disease. DL has been utilized independently to forecast eye or cardiac

conditions. But coherence of heart and eye are not popularly used. Also, existing research only focuses on blood vessels to predict age, smoking status, and blood pressure of a patient by examining the eye.

Thus, a novel approach to using eye disease to predict the occurrence of heart disease was proposed. The heart condition known as CAD, or coronary heart disease, and the eye condition known as CRAO were selected for analysis in this work. The eye and heart features are taken as input for prediction of CAD and CRAO is carried out simulataneously using Improved DenseNet. Then, the coherence between eye and heart are calculated.

The main contributions can be given as,

- To predict the CRAO and CAD disease, a novel method called Improved DenseNet is proposed. Owing to limited or unbalanced data, the preprocessed input features are fed into a Generative Adversarial Network (GAN) for data augmentation after undergoing a median filter treatment. The GAN model produces an augmented dataset that has a significant amount of patient data in it. Therefore, Principal Component Analysis (PCA) was used to reduce the dimensionality of the feature set. The dataset produced by the GAN model is subjected to this PCA-achieved feature set dimensionality reduction before being fed into the Improved DenseNet predictive model.
- The steps for predicting the heart disease is similar to the steps used in CRAO.
- The percentage of positive and negative cases in coherence prediction is determined using the Pearson correlation coefficient following the prediction of both CRAO and CAD.
- This facilitates the doctors' ability to treat patients promptly and without interruption.

This is the arrangement of the work. Section II discusses the review of previous works in the literature. The suggested method for predicting heart disease from eye disease is described in Section III. Section IV included a discussion of the findings. Section V then presents the conclusion.

II. LITERATURE SURVEY

Eye Disease Prediction Using Deep Learning

A deep learning-based technique for focused ocular detection is introduced. In this work, the 5000 photos of the eight different fundus classes that comprise the ODIR dataset are classified using image classification algorithms, such as VGG-19[4].

Vision transformers (ViTs) and Deep Convolutional Neural Networks (DCNNs) were introduced with the purpose of detecting retinal diseases [5]. These models have shown promise, but because retinal lesions are complicated, there are still issues.

Hybrid approaches for the categorization of a dataset on eye illnesses that combine fusion algorithms and feature extraction [6]. To categorize CFP photos for the purpose of diagnosing eye diseases, three methods were developed.

As a deep learning model, convolutional neural networks (CNN) and transfer learning were developed [7] to differentiate between a normal eye and one that has glaucoma, cataract, or diabetic retinopathy. A high accuracy of 94% was attained in multi-class categorization using transfer learning.

CNN model for early eye illness detection was proposed [8]. Four categories are identified by this approach for human eyes: healthy, conjunctivitis, cataract, and trachoma.

For the purpose of identifying diabetic retinopathy using fundus photos, a thorough comparative analysis of six models based on Convolutional Neural Networks and Deep Neural Networks, namely simple CNN, VGG16, DenseNet121, ResNet50, InceptionV3, and EfficientNetB3, was advised [9].

Heart Disease Prediction Using Deep Learning

To detect cardiac disease, a detailed comparison should be made between the Long-Term Memory Network Model (LSTM), Convolutional Neural Networks (CNN), Recurrent Neural Networks (RNN), Densenet, and Bi-LSTM [10].

A study comparing the use of deep learning and machine learning techniques for the classification and prediction of cardiovascular diseases (CVD) was conducted [11].

An adaptive Deep Featured Adaptive Convolution Neural Network for early risk identification is proposed [12] as a component of an enhanced healthcare data analysis model (dense net convolutional neural network) for cardiovascular prediction.[13] combined deep neural networks with the embedded feature selection technique to create a heart disease prediction algorithm.

Heart Disease Prediction with Retinal Images

[14] described how to assess cardiovascular risk using retinal images and deep learning techniques. By reviewing the major accomplishments of the most recent state-of-the-art DL approaches in automated CVD diagnosis, this paper provides a novel viewpoint.

Fundus photos and optical coherence tomography angiography (OCTA) are other tools used to assess the health of the heart. OCTA was developed to diagnose retinal diseases such as diabetic retinopathy, glaucoma, age-related macular degeneration, and retinopathy [15].

Using only retinal fundus images, an artificial intelligence platform is being developed and its accuracy evaluated in order to ascertain the relative contributions of the various risk factors that contribute to the overall 10-year risk of cardiovascular disease (CVD) [16].

The advent of OCT angiography has made it possible to visualize intraretinal capillary networks without the use of contrast, which may be utilized to spot early indications of kidney, eye, and heart disease [17].

As discussed above, the existing works focus prediction of heart disease with retinal images not discussed about correlation between whether the person have eye disease may have heart disease vice versa.

III. METHODOLOGY

Timely detection of disease diagnosis is very important in every person's life. Early disease diagnosis can help to treat disease earlier. Cardiovascular illness stands as a prominent fatal ailment globally. Statistics vividly illustrate its severity by showcasing the proportion of global deaths attributed to heart attacks. Consequently, there exists an inherent urgency to forecast this condition in its early stages.

To make the heart disease prediction at earlier stage in non-invasive way, eye can be used as an indicator. The blood vessels in the eye can indicate the possibility of heart disease. When the patients have CRAO, they might have the possibility of CAD. This CRAO can be considered as warning signal for the CAD. People in these cases should be treated immediately. Therefore, there is a correlation between heart disease and eye disease in order to reduce the percentage of deaths from heart disease. CAD and CRAO are predicted paralleley. Then, the coherence rate between the heart and eye disease is found at the last step.

Central Retinal Artery Occlusion (CRAO)

There are a few eye diseases that affect us in adverse ways. In this work, Central Retinal Artery Occlusion is discussed in a detailed manner.

Signs and Symptoms

The following symptoms can be noticed in patients if they suffer from CRAO : 90% cherry-red spot, 39% pallor, 32% retinal arterial attenuation, 58% retinal opacity in the posterior pole, and 22% optic disk edema [18]. As a future stages, plaques, optic atrophy, and emboli can be found.

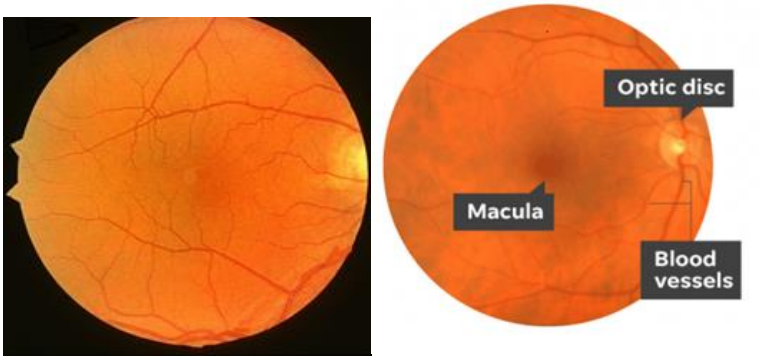

Fig 1. (a) Normal eye, (b) Eye with CRAO Symptoms.

Fig 1(a) shows the normal eye of the human without any disease. **Fig 1 (b)** indicates CRAO with symptoms like dark spot in the middle at back side of the eye in mascula region, bright spot at the right in the optic disc as well as change in blood vessels.

Diagnosis

With optical scattering media and micrometer-resolution, two- and three-dimensional images are captured with low-coherence light in Optical Coherence Tomography (OCT) imaging test. Using this test, retinal cross section images are captured with light waves. The distinctive layers of retina are analysed by ophthalmologist using OCT. They are measured and the thickness level is mapped which is very useful in diagnosis procedure.

Retinal whitening in an acute retinal artery occlusion is associated with severe inner retinal layer swelling from the ischemic event. A "cherry-red spot" in a CRAO is indicated by retinal whitening, thickening of the inner retinal layers, and normal fovea presence. As there is no inflammation of ganglion cells to hide the fovea, the fovea looks regular. The swelling / thickening of the inner retinal layers can be captured by OCT.

Coronary Artery Disease (CAD)

It is obvious that heart conditions have an impact on the other organs' ability to function normally because the heart is an important organ in the circulatory system. In this section, CAD is discussed in a detailed.

Signs and Symptoms

After completing food intake, doing regular tasks and other forecasted periods, chest pain may cause due to narrowed heart arteries. Sometimes, the symptoms occur like heartburn and also happened during excerise, stay for few seconds and get

cured by taking rest. It may sometimes occur without symptom. Mostly, it result in heart attack. Sometimes, heart failure or an abnormal heartbeat can be resulted.

Diagnosis
CAD can be diagnosed by the following tests.

Electrocardiogram
Electrocardiogram is a test carried out to monitor heart activity in a easy way.

Echocardiography
Sound waves are used in echocardiography to create images of the heart.

Stress Test
The stress test is recommended by doctor when symptoms and signs of coronary heart disease were found during exercise. Using treadmill, the patient are instructed to walk or drive an immobile cycle. It is termed as exercise stress test. The anomalous variations in the heart are observed by making workout in the test.

Coronary Angiography
Coronary angiography is recommended by doctor when other test results were found to be positive. This denotes that the patient has the possibility to have CAD. This test is carried out by injecting particular dye in coronary arteries via heart and it is termed as angiogram. A catheter is used for this task and it is made up of flexible thin tube. X-rays used for viewing blockages in the heart through dye.

The Eye and Heart Disease Relationship
Blood test are usually carried out to find the threat of cardiovascular disease by doctors. The aggressive techniques are utilized to carry out blood test and also it is time consuming. So, to make less aggressive, relaxed and quicker, retinal examination can be used to analyse heart with deep learning approach.

The overview of patient health can be represented by rear interior wall of the eye (also known as fundus) which contains crowded blood vessels. The retinal fundal images denotes the blood vessels at the back of the eye. These blood vessels indicate the status of age, blood pressure, smoking, gender which leads to cardiac disease. Then these factors can be used for cardiovascular disease prediction.

Having cardiovascular disease or an issue with a heart valve might hinder the efficient blood flow to your body's tissues and organs. Reduced oxygen supply to organs, including the eyes, can cause various signs and symptoms. This underscores the importance of a thorough eye examination for your overall health.

The ocular abnormalities listed below may be a sign of heart disease. Changes in blood vessels in the Eyes.

- Deposits of cholesterol in or near the eyes.
- Transient vision loss etc.,

Proposed Methodology

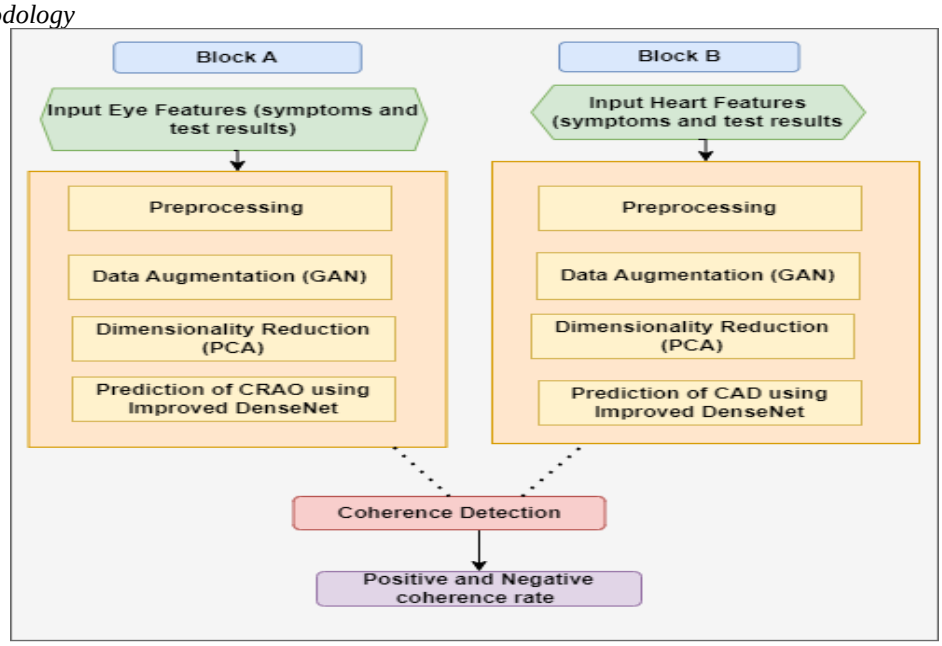

Fig 2. Pipeline of Workflow

Fig 2 represents the pipeline of overall workflow. In our proposed method, the symptoms and test results of CRAO are taken as input. Preprocessing is done to reduce noise in images using Median filter. The preprocessed input features are used for data augmentation using a Generative Adversarial Network (GAN) due to insufficient or unbalanced data. The GAN model generates augmented data that contains a large amount of patient data. To decrease the dimensionality of the feature set, Principal Component Analysis (PCA) was performed. Before feeding the dataset produced by the GAN model into the Improved DenseNet predictive model, the dimensionality of the feature set was reduced through PCA. The steps involved in the prediction of heart disease are similar to those in CRAO. Following the prediction of both CRAO and CAD, the percentage of positive and negative cases in coherence prediction is determined using the Pearson correlation coefficient.

Block A: Prediction of CRAO with Improved DenseNet

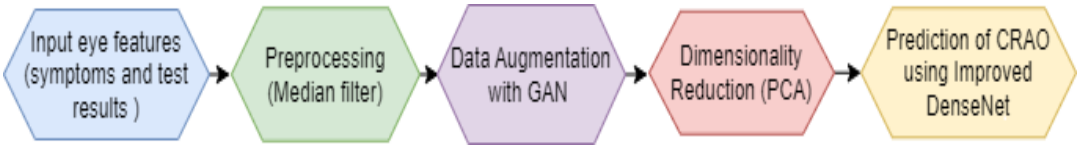

Fig 3. Work Flow of Block A.

Fig 3 shows, steps that are involved in Block A.

Data Representation

For CRAO eye disease prediction, we have collected a dataset of OCT test (Optical Coherence Tomography) for 25 patients from private hospital in India. OCT has the capability to record the thickening/swelling in the layers of the inner retina. Due to its common procedure in medical imaging, 30 million OCT scans are carried out every year globally.

Pre-Processing

First step in this process is pre-processing. Employing conventional image processing methods, such as Gaussian blur or median filtering, proves instrumental in noise reduction prior to the integration of images into a deep learning model. To preserve significant image details, typically those close to the edges, the median filter, for instance, replaces a pixel's value with the median of the values it covers with a filter mask [19].

$$(a, b) = \{g(i, j)\}, i, j \in Sab \tag{1}$$

Let Sab denote a collection of rectangular subimages centered at (a,b) and having a window size of (m*n).

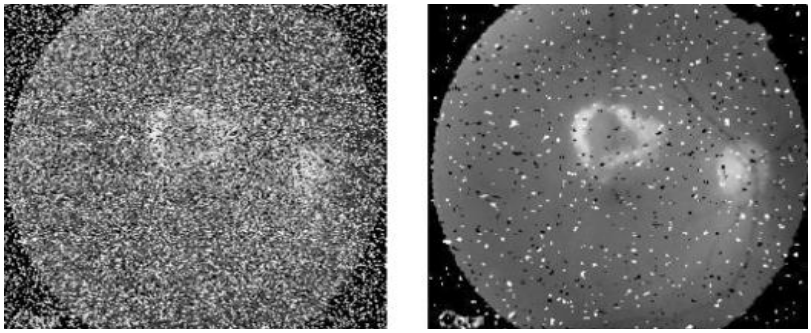

Fig 4. (a) Noisy Image vs (b) Median Filtered Image [20].

Fig 4 shows **(a)** Noisy Image vs **(b)** Median Filtered Image [20].

Data Augmentation

A dataset with limitations or imbalances can lead to an overfit model, leading to reduced prediction accuracy when applied to new data. Overfitting occurs when models excel in training but struggle with unseen test data. To tackle this challenge, the application of Generative Adversarial Network (GAN) [21] is considered.

The GAN operates as a dual-network framework comprising a generator and a discriminator. These networks engage in simultaneous competition and collaboration. Through numerous training iterations, the generator network learns to create synthetic data resembling real data, while the discriminator identifies this synthetic data as authentic. Once generated, the fake data can be incorporated with actual data for training and prediction within the proposed Improved Densenet model.

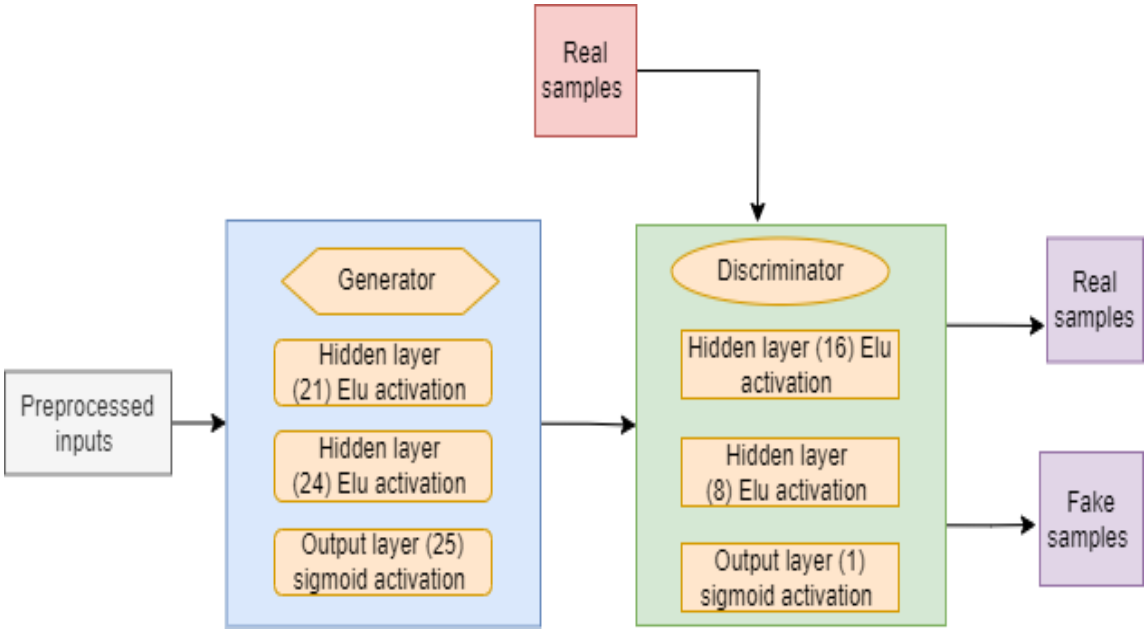

Fig 5. Block Diagram of GAN.

Fig 5 shows that block diagram of GAN [21]. In this model, the generator network is composed of three different layers. Equation (2) represents the first hidden layer, which is comprised of 21 neurons with an Elu activation function. is fed input data that includes CRAO test results and symptoms. After that, the second hidden layer employs an Elu activation function and has a total of 24 neurons. The output layer, which is the last layer in the generator network, is in charge of creating the synthetic samples. This layer comprises twenty-five neurons and uses a sigmoid activation function. Following their generation, the synthetic samples are combined with the original dataset and fed into the discriminator network, which shares three layers with the generator.

$$z = \begin{cases} x & when\ x \geq 0 \\ \alpha(e^{x} - 1) & when\ x < 0 \end{cases} \quad (2)$$

The dependent variable, z, is the function's output, while the independent variable, x, is controlled by the variable α, which determines the point at which the negative Elu component reaches saturation.

The real dataset and the synthetic samples are fed into the discriminator network, which has three distinct layers and a similar structure, after they have been assembled. A function called Elu activation functions sixteen neurons in the first hidden layer. The Elu activation function is also used by eight neurons in the layer below. Finally, a single neuron in the output layer uses a sigmoid activation function to discern between real and fake data.

Dimensionality Reduction Method

The dataset generated by the GAN model presents processing challenges due to its large number of features. It contains a substantial amount of patient data. These features include potential overfit elements for classification along with specific information related to heart and eye diseases. To manage this complexity, the dimensionality of the feature set was reduced using Principal Component Analysis (PCA) [21].

Steps for PCA Algorithm

- Normalize the data: Normalizing the data is the first step in preparing it for PCA. This involves ensuring that each variable has a mean of 0 and a standard deviation of 1.
- Compute the covariance matrix: Following normalization, the subsequent step entails computing the covariance matrix of the standardized data. This matrix reveals the relationships between each variable within the dataset.
- Determine the eigenvalues and eigenvectors: These eigenvectors signify the primary directions of data variance, while the eigenvalues denote the extent of variance along each eigenvector.
- Select the principal components: Identify the principal components by choosing the eigenvectors associated with the highest eigenvalues. By illustrating the primary directions of the greatest data variance, these elements help to decrease the dimensionality of the original data.
- Perform data transformation: Finally, convert the original data into the principal components' reduced-dimensional space.

Prior to inputting into the Improved DenseNet model, the dimensionality of the feature set within the dataset produced by the GAN model was decreased. This reduction not only diminished the number of crucial features supplied to the predictive models but also reduced the time required for training and prediction.

The Proposed Improved Densenet

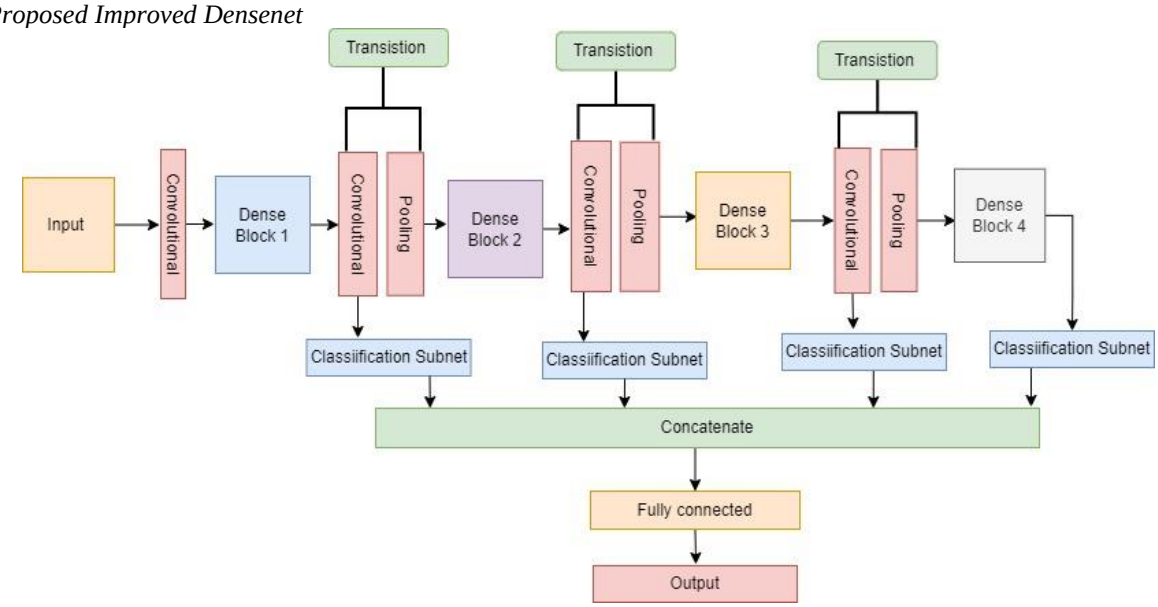

Fig 6. Improved DenseNet Architecture.

Fig 6 represents the block diagram of Improved DenseNet Architecture. Following dimensionality reduction, the data is directed to the Improved DenseNet [23] to forecast CRAO. Our proposed network architecture employed DenseNet-121, featuring direct connections between each layer in a feed-forward manner. This architecture consists of four dense blocks, three transition layers, and 121 layers (117 convolutional, 3 transition, and 1 classification). Slight adjustments were made to the DenseNet-121 structure in comparison to the standard model to improve CRAO prediction; however, further fine-tuning is necessary for optimal performance.

The convolutional layer that came after Dense Block 4 as well as the final pooling and linear layers were left out. Instead, the output of Dense Block 4 and the feature-map of each transition layer were routed to the relevant classification sub-networks. In this proposed CNN architecture, a rectified linear unit (ReLu), a convolution, and a convolution (Conv) are arranged after a batch normalization (BN) as the first convolution layer. The Conv layer employed a 7 × 7 filter matrix with a stride of 2.

By using the output from this convolution layer as the input for the Dense Block in the DenseNet, information flow between the layers is enhanced. A pooling layer and a convolution layer are also part of the transition layer.The convolutional output traverses the classification sub-network. To enhance feature extraction, the four basic building block iterations—Dense Blocks, transition layers, and classification sub-networks—were arranged in a sequential manner. The combined outputs from each building block were sent to the last fully connected layer.

Further information about the suggested enhanced Densenet framework will be provided in the sections that follow.

The Dense Block

A crucial component of the DenseNet [23] for enhancing the information flow between layers is the Dense Block. 3 x 3 Conv, BN, and ReLu comprise this structure. The particular formula looks like this:

$$X_n = H_n[X_0, X_1, \ldots\ldots, X_{n-1}] \tag{3}$$

Since Hn(.) is a composite function of three successive operations on the input of the n^{th} layer, $[X_0, X_1, \ldots\ldots, X_{n-1}]$ refers to the concatenation of the feature-maps created in layers 0,1,...,n−1.

Transition Layer

This transition layer, which is seen here between two thick blocks, modifies the size of the feature maps. It is made up of a 2 × 2 average pooling layer, a 1 × 1 convolution, a ReLu, and a BN. Convolution analyzes features by using properties from the layer that came before it. A convolution kernel, also known as a filter, composed of a set of weights, unites the extracted features. To become more nonlinear, all local weight values must pass through an activation function (such as the sigmoid or ReLU). One method to express the convolution process is as follows:

$$y^l = v^l . f_1 \left(y^{(l-1)} \right) + b^l \quad (4)$$

where fl(.) is the activation function and $y^l$is the l^{th} -layer neuron status. The weight matrix and bias are represented by. v^l and b^l respectively, from ($l-1)^{th}$to the l^{th}.

The purpose of the pooling layer is to reduce each feature map's dimensionality while maintaining crucial data. Both average pooling and max pooling techniques are used in our approach. In order to perform max pooling, a spatial neighborhood, like a 2 × 2 window, must be defined. The largest element within that window will then be extracted from the rectified feature map. On the other hand, when using average pooling, all of the elements within the window's average are calculated rather than just the largest one. For max pooling and average pooling, a 2 stride and a 3 × 3 window are used in the experiments, respectively.

The Sub-Network for Classification

To simplify the parameters, the classification sub-network is composed of a global average pooling algorithm, batch normalization (BN), and a softmax function.

By combining spatial information, global average pooling strengthens the input's resistance to physical translations. This pooling method transforms feature maps into statistics, reducing the risk of overfitting at this stage. Subsequently, batch normalization is applied to expedite training and stabilize the training process.

In this network, an input vector K of real numbers is processed by the softmax classifier, which normalizes the outputs to a sum of 1. The following formula defines the standard (unit) softmax functions σ: RK → RK:

$$\sigma(y)_j = \frac{e^{y_j}}{\sum_{k=1}^{k} e^{y_k}} \; j = 1, \ldots\ldots, k \; y = (y_1, \ldots\ldots, y_k) \in R^k \quad (5)$$

- The probability that the input belongs to class j is represented by $\sigma(y)_j$.
- The exponential of the raw score for class j is denoted by e^{y_j} . Greater scores are assigned more weight when the values in the input vector are amplified.
- $\sum_{k=1}^{k} e^{y_k}$ represents the sum of the exponentiated scores over all classes, which serves as the normalization factor. It ensures that the probabilities sum to 1, making it a valid probability distribution.

The Loss Function

To evaluate how well a classification model generates probability values between 0 and 1, we choose to use cross-entropy as our loss function. The following is the expression of this loss function, which increases when the predicted probability differs from the true label:

$$loss = -(clog(p) + (1-c)\log(1-p)) \quad (6)$$

In this case, 'p' denotes the expected probability and 'c' denotes the accurate classification. Our goal is to continuously reduce this loss value by training the network.

Block B: Prediction Of CAD Using Improved Densenet

Data Representation

The same 25 patients (those with eye diseases) were gathered as a dataset for the purpose of predicting coronary heart disease. The patients' age, gender, maximal heart rate, type of chest pain, exercise-induced ST depression, resting blood pressure, resting electrocardiogram outputs, and serum cholesterol in milligrams per deciliter were all included in this dataset.

The Improved DenseNet is used in this section to predict heart disease. Similar to the steps in Block-A are the steps for predicting heart disease. The percentage of positive and negative cases has been computed following the prediction of both CRAO and CAD.

Coherence Detection

The final stage in the prediction of heart disease is called coherence detection. By calculating the percentage of positive cases of corresponding heart and eye diseases, the coher ence relationship between CRAO and CHD is determined. By analyzing, the percentage of coherence is detected, which specifies the number of heart disease possibility due to eye disease. The positive coherence rate and negative coherence rate are determined at last. Positive coherence indicates the correct prediction and negative coherence indicates the false prediction of heart disease from eye disease.

The correlation coefficient can be used to determine how strongly two continuous variables are linearly related to one another. It displays the distance between data distribution points and a straight line. According to a positive correlation coefficient, when one variable rises, the other also tends to rise, and vice versa. Pearson's correlation [24] can be used to calculate the correlation value, as stated in equation (7). The following computation is made using this method, which specifically finds the linear relationship between two variables:

$$r_{xy} = \frac{n\sum x_i y_i - \sum x_i \sum y_i}{\sqrt{n\sum x_i^2 - (\sum x_i)^2}\sqrt{n\sum y_i^2 - (\sum y_i)^2}} \quad (7)$$

In which, The Pearson correlation coefficient between variables x and y is indicated by the symbolr_{xy}. N represents the total number of observations. x_i denotes the i th observation value of x and y_i denotes the i th observation value of y.

A perfect positive linear relationship, or one in which the increases of one variable are directly proportionate to the increases of the other, is indicated by a correlation coefficient of r = 1. On the other hand, a perfect negative linear relationship, denoted by r = -1, shows that as one variable rises, the other falls proportionately. The variables are said to be weakly or not strongly related when r ≈ 0, which denotes minimal to no linear relationship.

IV. RESULTS

Performance Evaluation

The measurement of Accuracy can be alternatively depicted through a confusion matrix, which showcases the count of accurately classified examples along the diagonal and misclassified instances in other cells. Below, **Table 1** presents the confusion matrix for the Improved DenseNet architecture.

Table 1. Confusion Matrix

N=25	Predicted Positive	Predicted Negative
Actual Positive	13	2
Actual Negative	2	8

When there is an imbalance in the dataset, an accurate evaluation of the architecture's performance might not be possible if accuracy is the only factor considered. As a result, the performance evaluation process also takes into account additional metrics like precision, recall, F1 Score, and the area under the ROC curve (AUC).

The model's performance is evaluated using the metrics that Kruthika et al. (2019) proposed: precision, recall, accuracy, and F1 score. To calculate accuracy, these metrics use True Positive (TP), True Negative (TN), False Positive (FP), and False Negative (FN).

Precision indicates the correct predicition of disease and it is represented by below formula (Kruthika *et al.*, 2019),

$$Precision = \frac{TP}{TP+FP} \quad (8)$$

Recall indicates the capability to identify the disease and it is represented by below formula,

$$Recall = \frac{TP}{TP+FP} \quad (9)$$

F1 score indicates the test accuracy measurement and it considers precision and recall. It is represented by below formula,

$$F1\ score = \frac{2TP}{2TP+TP+FP} \quad (10)$$

Accuracy indicates the probability of both correct positive and negative predicition. It is represented by below formula,

$$Accuracy = \frac{TP+TN}{TP+TN+FP+FN} \quad (11)$$

The ROC curve illustrates the relationship between the true positive rate and the false positive rate. The ROC curve for our suggested architecture closely resembles the ideal curve, demonstrating the architecture's excellent test-set performance.

True Positive (TP) in the example above denotes a patient whose test results are positive and who has both CRAO and CAD. False Positive (FP) refers to a patient's positive test result despite having CRAO but no CAD. True Negative (TN) denotes a patient with CRAO who also has CAD and a negative result. False Negative (FN) denotes a patient with CAD and CRAO when the test results are negative.

Training Accuracy

Based on the training data, the model's performance is reflected in the training accuracy [25]. The plotted graph showcases accuracy across each epoch. It's evident that as epochs progress, the model's accuracy consistently improves. In this case, the highest training accuracy stands at 97.2%. This high training accuracy signifies that the model adeptly learns parameters, resulting in minimal misclassification, as depicted in **Fig 7**.

Validation Accuracy

Testing accuracy, sometimes referred to as validation accuracy, is the accuracy determined on a dataset that the model hasn't been exposed to during training. This is a brand-new dataset that the model uses to gauge how well it can generalize. Generally speaking, validation accuracy ought to be at least as high as training accuracy. The plotted graph illustrates the validation accuracy across each epoch, revealing a slightly higher accuracy (97.5%) than the training accuracy. This suggests the model's proficiency in classifying a greater number of correct cases, as depicted in **Fig 7**. **Table 2** shows Comparison of Training and Validation Accuracy with Epochs.

Table 2. Comparison of Training and Validation Accuracy with Epochs

Epochs	Training accuracy	Validation accuracy
0	0.801	0.825
50	0.910	0.921
100	0.953	0.941
150	0.954	0.952
200	0.932	0.963
250	0.960	0.964
300	0.930	0.941
350	0.956	0.951
400	0.962	0.960
450	0.972	0.975

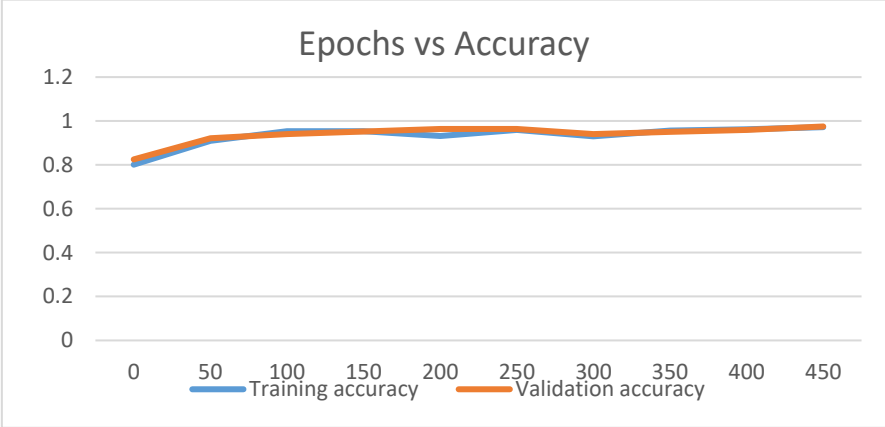

Fig 7. Training and Validation Accuracy.

The comparison of validation and training accuracy over different epochs is shown in **Fig 7**. After training Improved DenseNet 121 for 450 epochs, we obtained a training dataset accuracy of 0.972 and a validation dataset accuracy of 0.975.

Training Loss

Training loss reflects the error encountered within the training data. A model achieving perfect predictions would exhibit a loss of zero. Conversely, higher loss values indicate imperfect predictions. The primary objective of model training is to identify a set of weights that minimizes this loss. In observing the loss across epochs, an increasing number of epochs correlates with a reduction in loss. A lower loss signifies higher accuracy, indicating fewer errors in predicting CRAO and CAD cases, as depicted in **Fig 8.**

Validation Loss

Validation loss closely mirrors training loss but is calculated specifically on the validation set. When validation loss surpasses training loss, it signifies potential overfitting in the model. Similar to training loss, lower validation loss is desirable, although a slight degree of overfitting might be acceptable. The depicted plot illustrates validation loss across epochs, showcasing a decline as the number of epochs increases in **Fig 8**. This validation loss metric informs us about the model's prediction errors for CRAO and CAD in the test data. Lets fix, the iterations = 450, batch size number D=64, embedding D=1, hidden size D =64, layers D= 2, output size D =3, learning rate (D) is 0.0001. The model is saved with minimal validation loss. **Table 3** shows Comparison of Training and Validation Loss with Epochs.

Table 3. Comparison of Training and Validation Loss with Epochs

Epochs	Training loss	Validation loss
0	1.05	1.170
50	0.150	0.160
100	0.152	0.115
150	0.155	0.124
200	0.125	0.175
250	0.112	0.055
300	0.102	0.043
350	0.042	0.022
400	0.034	0.024
450	0.029	0.028

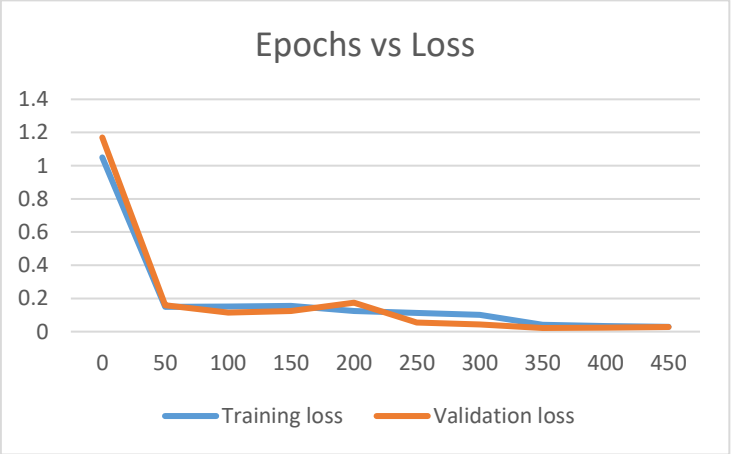

Fig 8. Training and Validation Loss.

After training 450 epochs for Improved DenseNet 121, we were able to obtain a 0.029 training loss and 0.028 loss in validation dataset. **Table 4** shows Performance Evaluation of Improved DenseNet, ResNet 50 and VGG 16.

Table 4. Performance Evaluation of Improved DenseNet, ResNet 50 and VGG 16

Models	Accuracy	Precision	Recall	F1-score	ROC
Improved DenseNet	97.50	95.47	94.08	95.97	95.80
ResNet 50 [26]	93.33	94.23	93.33	93.33	94.20
VGG 16 [26]	92	93.12	92.03	92.03	91.25

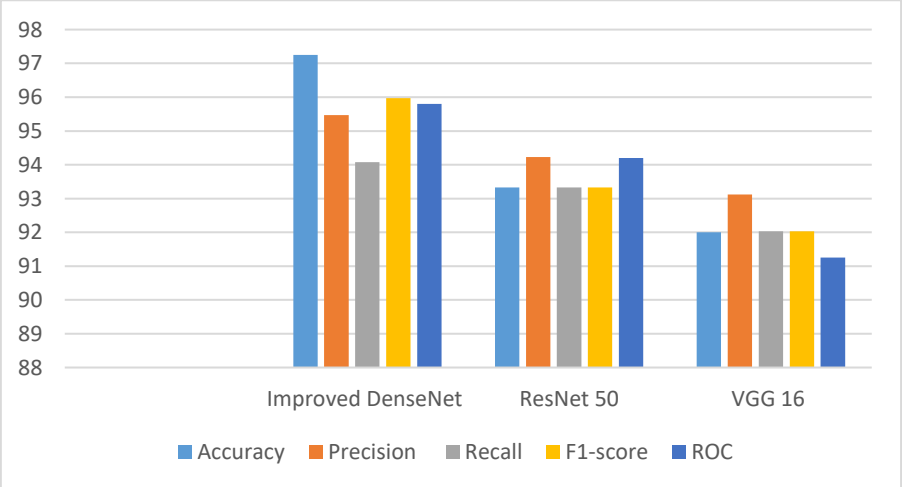

Fig 9. Performance Evaluation of Improved DenseNet, ResNet 50 and VGG 16.

The Improved DenseNet model underwent comprehensive evaluation to gauge its effectiveness in detecting CRAO and CAD. A number of metrics, including accuracy, precision, recall, F1-score, and ROC, that were derived from a confusion matrix were used to thoroughly assess the model. This evaluation's conclusion showed an exceptional accuracy of 97.50%, demonstrating its superior performance over other models. **Fig 9** shows Performance Evaluation of Improved DenseNet, ResNet 50 and VGG 16.

Discussion

The proposed method is illustrated by taking one sample patient eye image data. The eye image will be OCT test output. The proposed work is demonstrated using the OCT test results, Electrocardiogram, Echocardiography, Stress Test and Coronary Angiography test results of 25 subjects (people). Out of which, 10 subjects were affected by CRAO and CAD. The OCT test results of affected 10 subjects are shown in **Fig 10**. These affected subjects contain the cherry red spot in the OCT test scan indicating that the respective subjects are affected by CRAO disease.

The remaining 15 subjects results are normal. The proposed work's efficacy is demonstrated by contrasting the final outcomes with those of other methods like ResNet 50 and VGG 16. The images collected for the evaluation of proposed work are outlined in **Table 5** and **Fig 10** illustrates the sample dataset images of CRAO affected subjects. To demonstrate the proposed method, the one subject (sub1) details are taken who are affected by CRAO and CAD. Firstly, the OCT scan image of sub1 is taken and analysed. Following this, for the same sub1, the CAD prediction is carried out. Finaly, the Pearson's correlation coefficient between CRAO and CAD are analysed for the same subject to find the possibility of CAD.

Fig 10. Sample Image Dataset Affected By CRAO.

Table 5. Image Details

Total test images		Healthy images		Diseased images	
Eye	Heart	Eye	Heart	Eye	Heart
25	25	15	15	10	10

First, the sub1 OCT scan output image is taken and then pre-processed to remove unwanted noise as in **Fig 11**.

Fig 11. Subject1 OCT Scan Image.

The OCT image is then processed and turned into a grayscale image. Then, the converted grayscale image is analysed by the proposed system. **Fig 12** shows Grayscale Image.

Fig 12. Grayscale Image.

The proposed system detect changes in blood vessels, cherry red spot on the fovea (appears after certain period due to blockage of retinal artery), pallor near the optic disc in the OCT scan as illustrated in **Fig 13**.

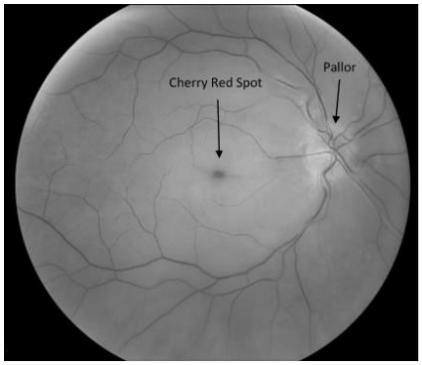

Fig 13. Final Output.

Fig 13 indicates the cherry redspot near the fovea and the change in blood vessels and pallor near the optic. This confirms that the sub1 is affected due to CRAO.

Next, the heart disease is predicted by taking the Electrocardiogram, Echocardiography, Stress Test and Coronary Angiography test results for the sub1. As the first three results turned to be positive for the sub1, the Coronary Angiography test result is taken and its output is evaluated as shown in **Fig 14.**

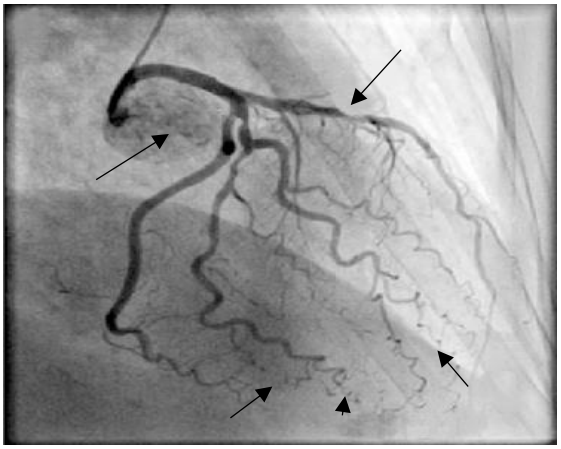

Fig 14. Coronary Angiogram of Subject1.

The abnormal narrowing of a passage in the left coronary arteries and the formation of wide links at the heart's apex are indicated by the black arrows. This indicates the sub1 has been suffered from CAD. **Table 6** shows Comparison Of Correlation of Proposed Model With Existing Models.

Table 6. Comparison of Correlation of Proposed Model With Existing Models

Correlation	Improved DenseNet	ResNet 50	VGG-16
Pearson correlation p-value for image 1	0.818	0.782	0.421

Table 7. Representation of Possibility of CAD from CRAO

OCT Image of Patient	True result of patient	Improved DenseNet	ResNet 50	VGG-16
Img1	Subject affected by CAD and CRAO	✓	✓	×
Img2	Subject affected by CAD and CRAO	✓	×	✓
Img3	Subject affected by CAD and CRAO	✓	✓	✓
Img4	Subject affected by CAD and CRAO	✓	×	×
Img5	Subject affected by CAD and CRAO	×	✓	×
Img6	Subject affected by CAD and CRAO	×	✓	✓
Img7	Subject affected by CAD and CRAO	✓	✓	×
Img8	Subject affected by CAD and CRAO	✓	✓	✓
Img9	Subject affected by CAD and CRAO	✓	×	✓
Img10	Subject affected by CAD and CRAO	✓	×	✓

In **Table 7**, the tick mark (✓) indicates p-valve more than 0.5, that shows the correct prediction of disease and cross mark (×) indicates the p-valve less than 0.5, that shows the wrong prediction of disease by the prediction methods. The images mentioned in the table denotes the patient who are affected by CRAO is also affected by CAD.

In above table, the proposed work correctly predicted 8 results out of 10. When compared to other techniques like CRAO and CAD, the proposed work accurately predict the possibility of CAD when a subject is affected by CRAO. The subject1 is in severe state because the patient has 80% symptoms like cherry red spot, pallor near opic disc and reduced blood vessels in the OCT output scan. This indicates the subject1 is affected by CRAO. And in **Fig 14**, the passage of arteries get narrowed indicating that the subject1 is affected from CAD.

For the entire dataset, the coherence relationship between CRAO and CAD is computed using Pearson's correlation coefficient. As was previously mentioned, 10 of the 25 patients had both CRAO and CAD. The stronger the relationship between the elements, the higher the P value. There is a significant correlation between the given CRAO and CAD variables if the P value is high.This indicates that the patient who suffered from CRAO also have CAD. As the proposed system predicts the 8 results correctly out of 10, the positive coherence rate is 80 percent and negative coherence rate is 20 percent. This proves that the proposed system is efficient in detecting the coherence rate in accurate manner.

V. CONCLUSION

To detect anomalies in heart conditions and to save human life, analysing health related heart data will be useful. Predicting heart disease is very difficult in medical area. Also, early diagnosis with preventive measures should be implemented and it will be helpful to control the death rate. Therefore, the Improved DenseNet model is suggested in this work to predict CRAO and CAD. The proposed approach is found to be accurate in disease predicition with high prediction accuracy of 97.50% when compared to existing methods. Furthermore, an 80 percent coherence rate between CRAO and CAD is found, suggesting that the suggested work is effective in determining the coherence relation.

CRediT Author Statement

The authors confirm contribution to the paper as follows:

Conceptualization: Nancy Lima Christy S and Nithyakalyani S; **Methodology:** Nithyakalyani S; **Software:** Nancy Lima Christy S; **Data Curation:** Nithyakalyani S; **Writing- Original Draft Preparation:** Nancy Lima Christy S; **Visualization:** Nancy Lima Christy S and Nithyakalyani S; **Investigation:** Nancy Lima Christy S; **Supervision:** Nithyakalyani S; **Validation:** Nancy Lima Christy S and Nithyakalyani S; **Writing- Reviewing and Editing:** Nancy Lima Christy S and Nithyakalyani S; All authors reviewed the results and approved the final version of the manuscript.

Data Availability

No data was used to support this study.

Conflicts of Interests

The author(s) declare(s) that they have no conflicts of interest.

Funding

No funding agency is associated with this research.

Competing Interests

There are no competing interests

References

[1]. National Center for Health Statistics. Multiple Cause of Death 2018–2021 on CDC WONDER Database. Accessed Feb 2, 2023.

[2]. "Correction to: Heart Disease and Stroke Statistics—2023 Update: A Report From the American Heart Association," Circulation, vol. 147, no. 8, Feb. 2023, doi: 10.1161/cir.0000000000001137.

[3]. World heart report 2023 https://world-heart-federation.org/wp-content/uploads/World-Heart-Report-2023.pdf.

[4]. M. S. Khan et al., "Deep Learning for Ocular Disease Recognition: An Inner-Class Balance," Computational Intelligence and Neuroscience, vol. 2022, pp. 1–12, Apr. 2022, doi: 10.1155/2022/5007111.

[5]. S. Muchuchuti and S. Viriri, "Retinal Disease Detection Using Deep Learning Techniques: A Comprehensive Review," Journal of Imaging, vol. 9, no. 4, p. 84, Apr. 2023, doi: 10.3390/jimaging9040084.

[6]. A. Shamsan, E. M. Senan, and H. S. A. Shatnawi, "Automatic Classification of Colour Fundus Images for Prediction Eye Disease Types Based on Hybrid Features," Diagnostics, vol. 13, no. 10, p. 1706, May 2023, doi: 10.3390/diagnostics13101706.

[7]. T. Babaqi, M. Jaradat, A. E Yildirim, S. H Al-Nimer, & D. Won, "Eye disease classification using deep learning techniques," (2023), In arXiv [cs.CV]. http://arxiv.org/abs/2307.10501.

[8]. B. Sankara Babu, B. Mandapati, B. Mandapati, H. Nallapu, P. Samanta, and K. Maithil, "Performance Comparison of CNN and DNN Algorithms for Automation of Diabetic Retinopathy Disease," E3S Web of Conferences, vol. 430, p. 01075, 2023, doi: 10.1051/e3sconf/202343001075.

[9]. A. Jaiswal, M. Singh, and N. Sachdeva, "Empirical Analysis of Heart Disease Prediction Using Deep Learning," 2023 International Conference on Advances in Computing, Communication and Applied Informatics (ACCAI), May 2023, doi: 10.1109/accai58221.2023.10201235.

[10]. M. Swathy and K. Saruladha, "A comparative study of classification and prediction of Cardio-vascular diseases (CVD) using Machine Learning and Deep Learning techniques," ICT Express, vol. 8, no. 1, pp. 109–116, Mar. 2022, doi: 10.1016/j.icte.2021.08.021.

[11]. V. J, R. Rajalakshmi, J. J. Gracewell, S. Suganthi, R. Kuppuchamy, and S. S. Ganesh, "Deep Featured Adaptive Dense Net Convolutional Neural Network Based Cardiac Risk Prediction in Big Data Healthcare Environment," International Journal on Recent and Innovation Trends in Computing and Communication, vol. 11, no. 2s, pp. 219–229, Jan. 2023, doi: 10.17762/ijritcc.v11i2s.6065.

[12]. D. Zhang et al., "Heart Disease Prediction Based on the Embedded Feature Selection Method and Deep Neural Network," Journal of Healthcare Engineering, vol. 2021, pp. 1–9, Sep. 2021, doi: 10.1155/2021/6260022.

[13]. R. G. Barriada and D. Masip, "An Overview of Deep-Learning-Based Methods for Cardiovascular Risk Assessment with Retinal Images," Diagnostics, vol. 13, no. 1, p. 68, Dec. 2022, doi: 10.3390/diagnostics13010068.

[14]. N. Thillaiarasu, B. Dasari, M. A. Kumar, M. P. Sandhya, and J. Y. Krishna, "Design and Development of Computational Methodologies for Predicting Parkinson's Disease with Artificial Intelligence," 2023 IEEE Fifth International Conference on Advances in Electronics, Computers and Communications (ICAECC), pp. 1–6, Sep. 2023, doi: 10.1109/icaecc59324.2023.10560322.

[15]. H. R. H. Al-Absi, M. T. Islam, M. A. Refaee, M. E. H. Chowdhury, and T. Alam, "Cardiovascular Disease Diagnosis from DXA Scan and Retinal Images Using Deep Learning," Sensors, vol. 22, no. 12, p. 4310, Jun. 2022, doi: 10.3390/s22124310.

[16]. E. Vaghefi, D. Squirrell, S. Yang, S. An, and J. Marshall, "Use of artificial intelligence on retinal images to accurately predict the risk of cardiovascular event (CVD-AI)," Oct. 2022, doi: 10.1101/2022.10.12.22281017.

[17]. T. E. Farrah, B. Dhillon, P. A. Keane, D. J. Webb, and N. Dhaun, "The eye, the kidney, and cardiovascular disease: old concepts, better tools, and new horizons," Kidney International, vol. 98, no. 2, pp. 323–342, Aug. 2020, doi: 10.1016/j.kint.2020.01.039.

[18]. N. Padrón-Pérez, R. Aronés-Santivañez, S. Muñoz, J. Arruga, and L. Arias-Barquet, "Sequential bilateral retinal artery occlusion," Clinical Ophthalmology, p. 733, Apr. 2014, doi: 10.2147/opth.s56568.

[19]. A.Haldorai, B. Lincy R, S. M, and M. Balakrishnan, "An improved single short detection method for smart vision-based water garbage cleaning robot," Cognitive Robotics, vol. 4, pp. 19–29, 2024, doi: 10.1016/j.cogr.2023.11.002.

[20]. H. S. Vijaya, M. A. Jayaram, A. Gowda, and B. P.T., "A Comparative Study on Filters with Special Reference to Retinal Images," International Journal of Computer Applications, vol. 138, no. 5, pp. 36–41, Mar. 2016, doi: 10.5120/ijca2016908834.

[21]. R. R. Sarra, A. M. Dinar, M. A. Mohammed, M. K. A. Ghani, and M. A. Albahar, "A Robust Framework for Data Generative and Heart Disease Prediction Based on Efficient Deep Learning Models," Diagnostics, vol. 12, no. 12, p. 2899, Nov. 2022, doi: 10.3390/diagnostics12122899.

[22]. G. T. Reddy et al., "Analysis of Dimensionality Reduction Techniques on Big Data," IEEE Access, vol. 8, pp. 54776–54788, 2020, doi: 10.1109/access.2020.2980942.

[23]. X. Li, X. Shen, Y. Zhou, X. Wang, and T.-Q. Li, "Classification of breast cancer histopathological images using interleaved DenseNet with SENet (IDSNet)," PLOS ONE, vol. 15, no. 5, p. e0232127, May 2020, doi: 10.1371/journal.pone.0232127.

[24]. T. A. Munandar, S. Sumiati, and V. Rosalina, "Pattern of symptom correlation on type of heart disease using approach of pearson correlation coefficient," IOP Conference Series: Materials Science and Engineering, vol. 830, no. 2, p. 022086, Apr. 2020, doi: 10.1088/1757-899x/830/2/022086.

[25]. X. Yuan, L. Zhang, and S. Zhao, "DenseNet Convolutional Neural Network for Breast Cancer Diagnosis," Proceedings of the 2022 3rd International Conference on Artificial Intelligence and Education (IC-ICAIE 2022), pp. 197–202, 2023, doi: 10.2991/978-94-6463-040-4_30.

[26]. A. L. A and J. N, "A Deep Learning Framework for Automatic Cardiovascular Classification from Electrocardiogram images," Jan. 2023, doi: 10.21203/rs.3.rs-2413127/v1.